Lamb Waves in Composite Plates: Tuned Excitation and Diffraction by Obstacles

E. GLUSHKOV, N. GLUSHKOVA, A. EREMIN, R. LAMMERING
and M. NEUMANN

ABSTRACT

The paper is devoted to theoretical and experimental investigations of Lamb wave excitation and propagation in multilayered carbon fiber-reinforced plastic plates with obstacles. The theoretical modeling is performed in the context of general linear elasticity for three-dimensional laminate anisotropic media. It is based on the integral and asymptotic representations in terms of Green's matrix of the structure under consideration. Those representations allow one to carry out fast and reliable quantitative amplitude and energy analysis of guided waves excited by specific sources and diffracted by surface and internal obstacles. In the experimental procedures the Lamb waves are generated by piezoelectric wafer actuators and measured by a laser vibrometer; permanent magnets placed at both plate sides serve as obstacles.

The influence of material anisotropy and excitation frequency on spatial directivity of generated wave fields has been analyzed. In particular, the effect of frequency-dependent alternation of the main lobe of the guided wave radiation diagram has been revealed and experimentally verified. This phenomenon leads to a more complicated tuning procedure for optimal Lamb wave excitation since the optimal frequencies ("sweet spots") depend not only on the piezoactuator's shape and size but, in addition, on the direction of propagation. Source tuning with accounting for this effect leads to clearer diffraction patterns; this is illustrated by experimental examples.

_____

Evgeny Glushkov, Natalia Glushkova, Artem Eremin, Institute for Mathematics, Mechanics and Informatics, Kuban State University, Krasnodar, Stavropolskaya st., 149, 350040, Russia, E-mail: evg@math.kubsu.ru

Rolf Lammering, Mirko Neumann, Institute of Mechanics, Helmut-Schmidt-University/University of the Federal Armed Forces Hamburg, D-22043 Hamburg, Germany, E-mail: rolf.lammering@hsu-hh.de

INTRODUCTION

Many modern layered composite materials exhibit anisotropic mechanical properties due to the complexity of their internal structure. This circumstance results in more challenging problems for predictive simulation since the patterns of guided waves (GWs) generated in anisotropic structures are featured by additional spatial angular dependencies of dispersion and amplitude characteristics. In particular, even with an axially symmetric source, a focusing of wave energy transfer in certain directions of GW propagation from the source may occur.

It was experimentally and theoretically shown that with a point source, e.g., with a focused immersion transducer or with a laser generation, the directivity of GWs is specified by the fiber orientation in the composite unidirectional sublayers and such radiation patterns is weakly frequency dependent [1-3]. On the other hand, with a dimensional source the radiation patterns become more complex and strongly frequency dependent. Theoretical investigations of cross-ply laminates driven by circular piezoelectric actuators [3,4] have shown that with frequency or source diameter increase the main radiation lobe periodically alternates either along the upper-ply fibers or in the perpendicular direction. This effect can be theoretically explained through the in-phase or out-of-phase interaction of wave packages generated by the opposite actuator's edges. Thus, due to the angular variation of the mode wavelengths caused by the material anisotropy, the tuned frequencies ("sweet spot" [5]) become also angle dependent.

The present work aims at experimental verification of the effects predicted in the context of the theoretical model [3,6], first of all, of the influence of source and composite properties on the tuning frequencies, as well as at the demonstration how this information can be used in GW SHM.

THEORETICAL BACKGROUND

The theoretical modeling has been performed in the context of general linear elasticity for three-dimensional anisotropic solids. It is assumed that a laminate composite structure, fabricated from elastic transversely isotropic homogeneous sublayers with arbitrary ply orientation, occupies the domain $D : |x| < \infty, |y| < \infty, -H \leq z \leq 0$ in the Cartesian coordinates $\mathbf{x} = (x, y, z) = (x_1, x_2, x_3)$ (Fig. 1). The sublayers are perfectly bonded with each other. The outer sides of the waveguide $z = 0$ and $z = -H$ are stress-free except the contact area Ω, to which a circular piezoelectric actuator is attached, and the obstacle contact areas S_i. The radial stress $\tau_r(x, y)$ arises in Ω due to patch radial deformation under a driving electric field. In the frequency range of interest (below 500 kHz-mm) the latter are well approximated by δ-like traction of uniform magnitude distributed along the actuator perimeter $r = \sqrt{x^2 + y^2} = a$:

$$\mathbf{q} = \{\tau_r \cos\varphi, \, \tau_r \sin\varphi, -H\}, \quad \tau_r = \delta_r(r - a).$$

The contact stress $\mathbf{q}(x, y) \, e^{-i\omega t}$ causes the response of the structure $\mathbf{u}(\mathbf{x}, \omega) = \{u_1, u_2, u_3\}$ which obeys the elastodynamic equations in displacements

$$C_{ijkl} u_{l,jk} + \rho\omega^2 u_i = 0, \quad i = 1, 2, 3 \tag{1}$$

They hold in every sublayer with specific values of the elastic stiffness tensor components C_{ijkl} and material density ρ; $\omega = 2\pi f$ is angular frequency, f is frequency in kHz.
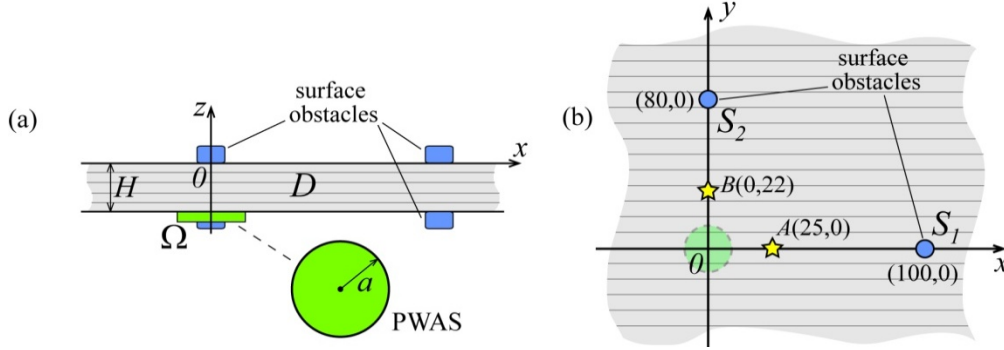

Figure 1. Geometry of the problem.

In the context of semi-analytical integral approach time-harmonic displacements $\mathbf{u}(\mathbf{x},\omega)$ are represented via the convolution of the Green's matrix $k(\mathbf{x},\omega)$ for the structure with the vector-function $\mathbf{q}$ that can be rewritten in terms of their Fourier symbols $K = \mathscr{F}_{xy}[k]$ and $\mathbf{Q} = \mathscr{F}_{xy}[\mathbf{q}]$:

$$\mathbf{u}(\mathbf{x}) = \frac{1}{(2\pi)^2} \int_{\Gamma_+} \int_0^{2\pi} K(\alpha,\gamma,z)\mathbf{Q}(\alpha,\gamma)e^{-i\alpha r\cos(\gamma-\varphi)}d\gamma d\alpha \qquad (2)$$

The Cartesian variables $\mathbf{x}$ and the Fourier parameters $\boldsymbol{\alpha} = (\alpha_1,\alpha_2)$ are taken in the cylindrical and polar coordinates (r,φ,z) and (α,γ); Γ_+ is the integration contour, going in the complex plane α along the real semi-axis $\operatorname{Re}\alpha \geq 0$, $\operatorname{Im}\alpha = 0$ and bypassing real poles $\zeta_n = \zeta_n(\gamma) > 0$ of the matrix K elements in accordance with the principle of limiting absorption.

The use of the residue technique and the stationary phase method brings explicit integral representation (2) to the asymptotic expansion in terms of guided waves $\mathbf{u}_n$:

$$\mathbf{u}(\mathbf{x}) = \sum_{n=1}^{N_r} \mathbf{u}_n(x) + O((\varsigma_n r)^{-1}), \ \varsigma_n r \to \infty \qquad (3)$$

$$\mathbf{u}_n(\mathbf{x}) \sim \sum_m \mathbf{a}_{nm}(\varphi,z)e^{is_{nm}r}/\sqrt{\varsigma_n r}$$

The amplitude factors $\mathbf{a}_{nm}$ are expressed via the residues of the product $K\mathbf{Q}$ from the real poles ζ_n; $s_{nm} = s_n(\gamma_m)$ are wavenumbers of the GWs $\mathbf{u}_n$, γ_m are the stationary points of the phase functions $s_{nm} = \zeta_n(\gamma_m)\sin(\gamma_m - \varphi + \pi/2)$: $s_n'(\gamma_m) = 0$; N_r is the number of real poles ζ_n. To constant factors the amplitude functions $\mathbf{a}_{nm}(\varphi,z)$ coincide with the GW modal eigenforms that may be derived using the modal analysis technique. The series expansion (3) provides a computationally efficient and physically clear analytically-based tool for GW analysis, which already accounts for the source influence on the host structure through the vector-function $\mathbf{Q}(\alpha,\gamma)$.

In the presence of surface obstacles the scattered wavefield $\mathbf{u}_{sc}(\mathbf{x}, \omega)$ is also representable in the form of Eq. (2) but with the unknown contact stress vector-function $\mathbf{q}_s(x, y)$. The latter can be obtained from the boundary integral equations arising from the substitution of the total displacement field into the boundary conditions in the obstacle contact area S_i [6]. In case of internal volumetric obstacles or corrosion the scattered field $\boldsymbol{u}_{sc}$ is obtained using the laminate element method [7].

EXPERIMENTAL SETUP

A uni-directional plate with the lay-up $[0^o]_4$ and dimensions $1000 \times 1000 \times 2.25$ mm^3 manufactured by Carbotec GmbH is used in the experiments. The material properties of transversely isotropic prepregs are the following: $C_{11} = 109.3$, $C_{22} = 13.8$, $C_{12} = C_{13} = 7.0$, $C_{23} = 5.8$, $C_{55} = C_{66} = 4.4$ (in GPa) and $\rho = 1500$ kg/m^3.

The plate is driven by a single circular vertically polarized piezoceramic actuator (PI Ceramic GmbH, PIC151 ceramic type) placed at its center (radius of the electroded area $a = 7.8$ mm, thickness $b = 0.25$ mm).

The velocity field of the propagating waves is captured on the opposite side of the plate by means of a Polytec PSV-400 scanning laser vibrometer and a Tektronix TDS 1012B two-channel digital storage oscilloscope. The scanning head of the PSV-400 system is placed 1.312 m above the specimen. A thin reflective film is glued to the surface of the plate in the area of observation, which is proved to be a suitable tool for improving the laser beam reflection and minimizing the signal-to-noise ratio.

The actuator is excited by a five-cycle Hann windowed sine tone-burst with a central frequency f_c and a repetition rate varying from 30 ms for low frequencies to 2 ms for the higher ones:

$$V(t) = \begin{cases} 0.5\sin(2\pi f_c t)(1 - \cos\dfrac{\pi f_c t}{5}), & 0 \le t \le 2T \\ 0, & t > 2T \end{cases}$$

For this purpose a Tektronix AFG 3022B two-channel arbitrary signal generator coupled with a Develogic WBHV 2A600 amplifier is used. To obtain the frequency response in various propagation directions the actuator is driven by a periodic chirp generated by the vibrometer hardware and covering the range from 10 kHz to 250 kHz. The fast Fourier transform is then applied to the measured signals.

Two powerful permanent magnets in the shape of cylinders serve as surface obstacles (diameter d=6 mm). They are fixed at both sides of the plate oppositely and can easily be removed or relocated to an arbitrary position.

RESULTS AND DISCUSSION

First, to reveal the influence of the material anisotropy and source dimensionality on the GW directivity, two points *A(25, 0, 0)* and *B(0, 22, 0)* (mm) in the directions along and across the fibers of the composite has been selected for the frequency response measurement and simulation (Fig. 1(b)). The plots of the out-of-plane velocity magnitude $|v_z| = \omega |u_z|$ measured at these points are shown in Fig. 2. The

curves exhibit alternations of minima and maxima which are typical for dimensional sources [5,6,8]. In contrast to the isotropic case [6], local minima and maxima of the curves do not generally occur simultaneously due to the difference in wavelengths along and across the fiber directions. Therefore, the optimal central excitation frequencies f_c are different for different propagation directions. The frequency points of local minima and maxima obtained theoretically are marked in Fig. 2 by diamonds (for point A) and dark circles (for point B). The marks on the upper and lower axes are for the maxima and minima, respectively. One can see a good agreement of the predicted and measured frequencies.
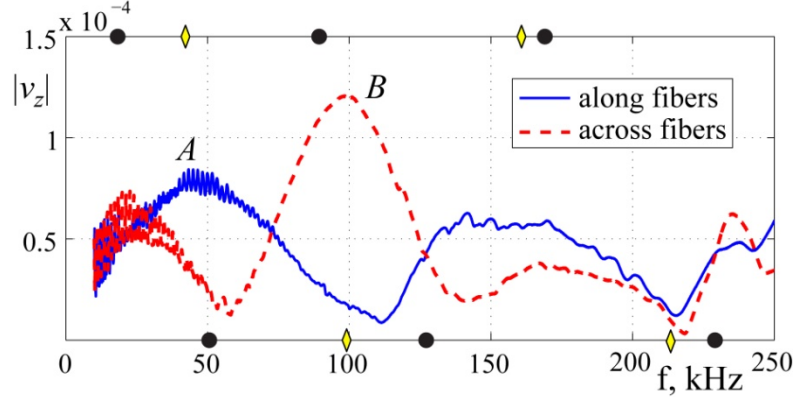

Figure 2. Frequency spectrum of the out-of-plane velocity amplitudes $|v_z|$ at the points A and B (experimental measurements).

To illustrate how the proper choice of f_c influences on wave propagation patterns, experimental and predicted transient out-of-plane velocities $\dot{u}_z(\mathbf{x},t)$ recorded 100 mm away from the source in the directions along and across the fibers are given in Fig. 3. As expected [6], the a_0 wave packages excited at the frequencies where local maxima of $|v_z|$ occur (subplots (a) and (c)) propagate without visible dispersion. On the contrary, wave packages in subplots (b) and (d) become blurred, splitting into two separate packages. It should be also noted that in the low-frequency range the maximum in one of the directions occur almost at the minimum of the counterpart one. Thus, selecting, for example, the frequency $f_c = 100$ kHz as a global optimum for the whole plate monitoring can lead to poor signal quality in the fiber direction.

As an example, Fig. 4 presents experimental transient out-of-plane displacements $u_z(\mathbf{x},t)$ at the point (40,0,0) mm for the plate with the surface obstacle S_1 recorded for two excitation frequencies $f_c = 50$ kHz (a) and $f_c = 100$ kHz (b). The reflected field pronounces itself as a second wave package arriving after the incident one. In the left subplot (a) its amplitude is quite distinguishable and separable from the incident waves, whereas in the right subplot (b) it is small and blurred.

Finally, though $f_c = 100$ kHz is optimal central frequency for the direction across the fibers, the reflected field is almost undetectable on a single-point time-history plot (Fig. 5, subplot (b)). On the other hand, the root-mean square (RMS) scan of the laminate surface displacements $u_z(\mathbf{x},t)$ exhibits typical diffraction patterns in the vicinity of the obstacle S_2, allowing one to identify its position. The reason of such a
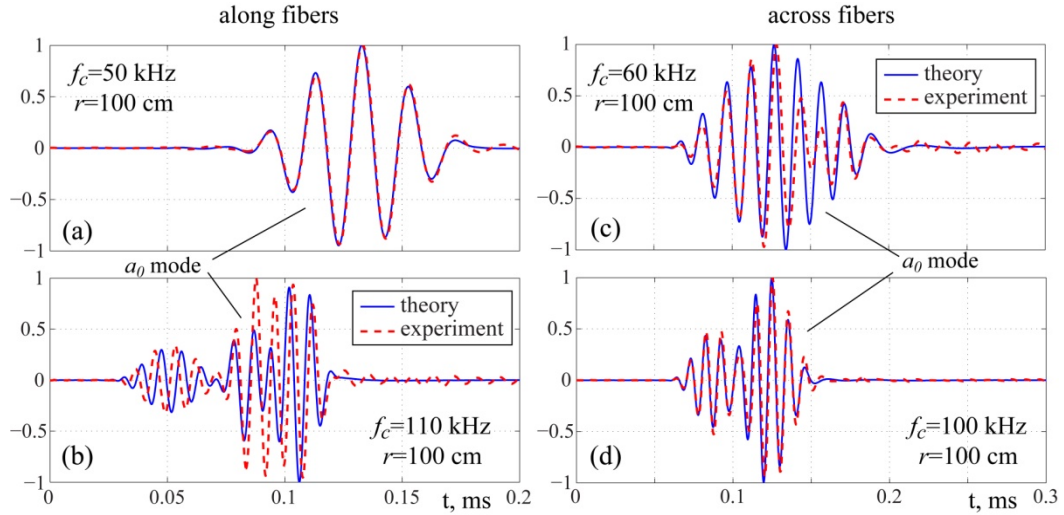
Figure 3. Influence of propagation directions and central excitation frequencies on the transient normalized velocities $\dot{u}_z(\mathbf{x},t)$.
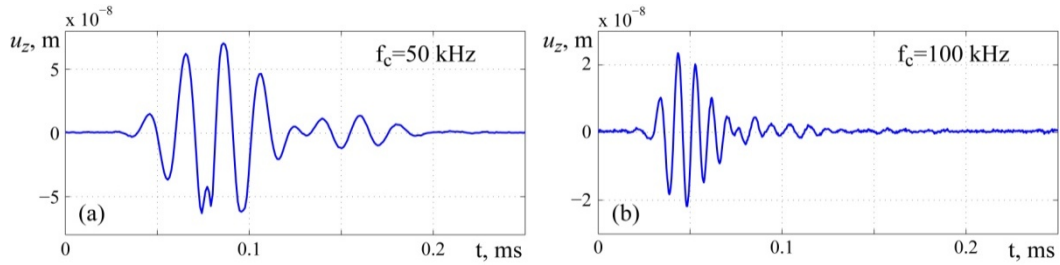

Figure 4. Experimental transient displacements $u_z(\mathbf{x},t)$ for the sample with the surface obstacle S_1 recorded at the point (40,0,0) mm (see Fig. 1).
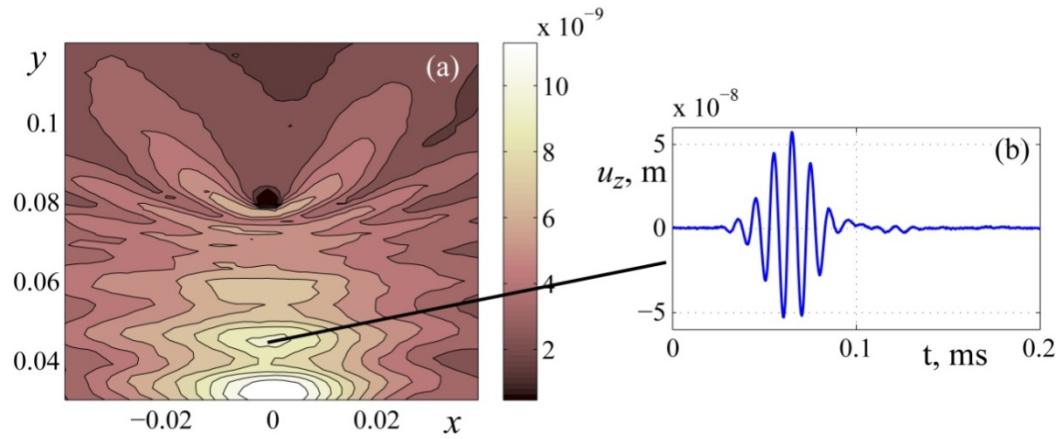

Figure 5. RMS of transient displacements $u_z(\mathbf{x},t)$ in the case of surface obstacle S_2 (a), and single point time-history (b) (point (0,45,0) mm).

behavior is a comparatively small amplitude of the backward a_0 mode reflected from this obstacle due to a strong damping in the direction across the fibers.

SUMMARY AND CONCLUSIONS

Strong frequency dependence of GW directivity in anisotropic layered composites actuated by a sized source has been theoretically predicted and experimentally validated. This effect should be accounted for a proper frequency tuning of Lamb wave based SHM and defect detection in composite plates.

REFERENCES

1. Balasubramaniam, K.; Krishnamurthy, C.V. (2006) "Ultrasonic guided wave energy behavior in laminated anisotropic plates", *Journal of Sound and Vibration*, Vol. 296, pp. 968–978.
2. Chapuis, B.; Terrien, N.; Royer, D. (2010) "Excitation and focusing of lamb waves in a multilayered anisotropic plate", *J. Acoust. Soc. Am.*, Vol. 127, pp. 198–203.
3. Glushkov, E.; Glushkova, N.; Eremin, A. (2011) Forced wave propagation and energy distribution in anisotropic laminate composites, *J. Acoust. Soc. Am.*, Vol. 129, pp. 2923–2934.
4. Nadella, K.S.; Salas, K.I.; Cesnik C.E.S. (2010) Characterization of guided-wave propagation in composite plates, *Proc. SPIE*, Vol. 7650, No. 76502H.
5. Giurgiutiu, V. (2008) "Structural Health Monitoring with Piezoelectric Wafer Active Sensors", Elsevier Academic Press, London.
6. Glushkov, E.; Glushkova N.; Lammering, R.; Eremin A., Neumann, M.-N. "Lamb wave excitation and propagation in elastic plates with surface obstacles: proper choice of central frequencies", *Smart Mater. Struct.*, Vol. 20, No, 015020.
7. Glushkov, Ye.V.; Glushkova, N.V.; Yeremin, A.A.; Mikhas'kiv, V.V. (2009) The layered element method in the dynamic theory of elasticity, *Journal of Applied Mathematics and Mechanics*, Vol. 73, pp. 449–456.
8. di Scalea, F.L.; Matt, H.; Bartoli, I. (2007) The response of rectangular piezoelectric sensors to Rayleigh and Lamb ultrasonic waves, *J. Acoust. Soc. Am.*, Vol. 121, No. 1, pp. 175–187.